ORNL/LTR-2014/487

A Model of Radiation-induced Microstructural Evolution

Alexander V. Barashev[1,2], Stanislav I. Golubov[2], and Roger E. Stoller[2]

[1]Center for Materials Processing
Department of Materials Science and Engineering
University of Tennessee, Knoxville, TN 37996-0750, USA

[2]Materials Science and Technology Division
Oak Ridge National Laboratory
Oak Ridge, TN 37831-6114, USA

Prepared for:

Light Water Reactor Sustainability Program
Office of Nuclear Energy, Science and Technology
U.S. Department of Energy

September 2014
Oak Ridge National Laboratory

Abstract

This report documents a comprehensive model that has been developed to enable simulations of microstructural evolution under the irradiation conditions typical of light water reactor (LWR) internal components. Although the model has been parameterized to account austenitic stainless steels, with suitable material parameters it should be applicable to other alloys as well. This report focuses on the details of the physical model and the computational implementation of the model. Representative results are included to illustrate the predictions of the model for swelling and dislocation evolution under LWR irradiation conditions. Additional applications and potential future developments for the model are also discussed.

In its current version, the code calculates dose dependence of swelling due to the nucleation and growth of an ensemble of cavities (bubbles or voids) under conditions of irradiation or thermal aging, the nucleation and growth of faulted dislocation loops, and the evolution of the network dislocation structure.

Contents

Abstract i

Nomenclature 1

1. Introduction 2

2. Description of the Physical Model 2

1.1. Equations 3

1.1.1. Master equations 3
1.1.2. Equation of state for helium in bubbles 4
1.1.3. Equations for mobile species 5
1.1.4. Sink strengths 6
1.1.5. Defect production rates 6
1.1.6. Gas atom generation rates 7
1.1.7.Generation of Frenkel pairs by over-pressurized gas bubbles 7
1.1.8. Network dislocation evolution 7
1.1.9. Correspondence between f_x and f_R 8
1.1.10. Grain boundary coverage 8

1.2. Geometry and boundary conditions 9

1.3. Integration method 9

1.3.1. Grouping scheme 9
1.3.2. Time integration 10

3. Typical Results of Simulations 11

4. Implementation of the Computer Model. 15

4.1 Description of Code Input 15

4.1. 1 An example of input file: `RIME_INPUT.dat` 15

4.2. Line-by-line description of the input file 17

4.2.1. Headline 17
4.2.2. Group of parameters defining the problem in general 18
4.2.3. Title of calculation 18
4.2.4. Volume or surface calculations 18
4.2.5. Irradiation or aging 18
4.2.6. New calculation or continuation of old calculation 18
4.2.7. On-the-fly control of calculation cell size 18
4.2.8. Cancelling nucleation 19
4.2.9. Time steps 19
4.2.10. Frequency of writing files 19
4.2.11. Group of parameters for Euler integration method 19
4.2.12. Group of parameters defining irradiation or aging conditions 20
4.2.13. Physical time 20
4.2.14. Description of defects production in cascades 20
4.2.15.Irradiation conditions and materials microstructure 20

4.2.16. Gas-atom production 20
4.2.17. Material properties 21
4.2.18. Reaction cross-sections 21
4.2.16. Gas bubble size distribution: vacancy part 22
4.2.17. Gas bubble size distribution: gas atom part 23
4.2.18. Interstitial and vacancy loops 23
4.2.19. Gas bubble size distribution: gas atom part 24

4.3. Additional input in '`module USER_mod`' 25

4.4 Description of Code Output 27

4.4.1. Output to screen 27
4.4.1. Example of the head at the beginning of calculations 27
4.4.2. Line by line explanation of the head of calculations 27
4.4.3. Example of the repetitive part for different irradiation/aging times 28
4.4.4. Line by line explanation of the repetitive part 29

4.5. List of output files in alphabetic order 32

4.6. Detailed description of the output files 32

4.7. Binary files used to save intermediate state for further calculation or restarts 36

4.7.1. zz_age_ct.dat: continuation of aging 36
4.7.2. zz_igr_ct.dat: surface irradiation after bulk irradiation 36
4.7.3. zz_irr_ct.dat: continuation of irradiation 36

5. Summary of Status and Future Work 37

References 38

Nomenclature

3-d – three-dimensional or three-dimensionally;
dpa – displacements per atom;
EOS – equation of state;
LSODE – Livermore solver for ordinary differential equations;
NRT – standard for calculating displacements per atom (after authors M. Norgett, M. T. Robinson, and I. Torrens);
ODE – ordinary differential equations;

1. Introduction

This is the fourth report on the modeling-based research of radiation-induced microstructural evolution in the austenitic stainless steels used to fabricate commercial light water reactor internal components. The overall objective of this task is to develop a predictive model that can be used in lifetime assessments of these components. This is relevant to component lifetime in the nominal initial license period of about 40 years and is particularly important for considering the extended licensing periods of interest to the Light Water Reactor Sustainability (LWRS) program.

The first three reports [1-3] focused on recent data which provided strong evidence of void swelling in austenitic stainless steels at temperatures below 350°C and discussed possible mechanisms that could explain this previously unexpected swelling. In addition to temperature and total dose, the displacement rate and helium generation rate are irradiation parameters of interest. Preliminary modeling work was carried out using a model developed previously for higher temperature irradiation conditions in fast reactors and the results were consistent with the experimental observations [1-2]. The primary shortcoming of the fast reactor model was its very limited and *ad hoc* cavity nucleation model. Therefore a more detailed cavity nucleation and growth model was developed and is described in [3]. Although that nucleation model is computationally more complex, it provides a much more rigorous description of the physical phenomena involved.

Subsequent effort has been focused on developing an integrated model of microstructural evolution that couples the high-fidelity cavity nucleation model with the dislocation evolution component from the previous fast reactor model. This integrated model is described in this report with a particular focus on the computational implementation of the model so that other researchers can make use of code. Although we have focused on the austenitic stainless steels of interest to the LWRS program, the basic model should be application to most steels and Ni-based alloys with appropriate parameterization.

2. Description of the Physical Model

The code performs numerical integration of the master equations for the size-distributions of gas bubbles and interstitial loops, coupled with equations for concentrations of the mobile species: single vacancies and-interstitial atoms, gas atoms, and both dislocation loops and the network dislocation density. A specially developed grouping scheme [4-8] and the double precision version of the Livermore solver for ordinary differential equations (DLSODE) [9-11] are used. The integration is performed in the (x, m) phase space, where x and m are the numbers of vacancies and gas atoms in a bubble, respectively. The output includes the dose dependence of the size distributions in the (x, m) and (R, m) phase spaces, where R is the gas bubble/loop radius, and integral characteristics of the microstructure, such as bubble and loop densities, bubble and loop mean sizes, swelling, and network dislocation density. The hardness or yield strength change associated with the microstructural evolution can be calculated using a standard dispersed barrier hardening model.

1.1. Equations

1.1.1. Master equations

The size distribution of gas bubbles $f_{x,m}$ obeys the following master equation (see Fig.1), which accounts for the reactions of bubbles with vacancies, interstitials and gas atoms, causing bubbles to grow/shrink and changing gas pressure in the bubble. The latter affects the surface energy, hence stability of the bubble to vacancy emission.

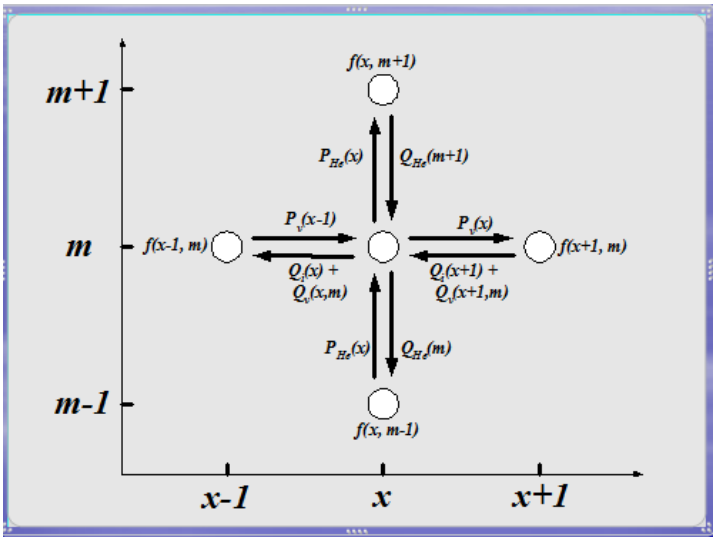

Fig. 1. Schematic diagram of reactions of mobile defects: vacancies, interstitials and gas atoms with (*x*, *m*) gas bubbles, where *P(x,m)* and *Q(x,m)* are the rates of corresponding reactions.

$$\begin{aligned}\frac{df_{x,m}}{dt} = {} & G_{x,m} - P^{\mathrm{i}}_{x,m} f_{x,m} + P^{\mathrm{i}}_{x+1,m} f_{x+1,m} \\ & - P^{\mathrm{v}}_{x,m} f_{x,m} + P^{\mathrm{v}}_{x-1,m} f_{x-1,m} - P^{\mathrm{g}}_{x,m} f_{x,m} + P^{\mathrm{g}}_{x,m-1} f_{x,m-1} \\ & - Q^{\mathrm{v}}_{x,m} f_{x,m} + Q^{\mathrm{v}}_{x+1,m} f_{x+1,m} - Q^{\mathrm{g}}_{x,m} f_{x,m} + Q^{\mathrm{g}}_{x,m+1} f_{x,m+1}\end{aligned} \quad . \tag{1}$$

Here $G_{x,m}$ is the generation rate of (*x,m*) clusters in cascades of atomic displacements. The association, *P*, and dissociation, *Q*, reaction rates for single vacancies (superscript v), interstitial atoms (superscript i) and gas atoms (superscript g) with gas bubbles containing *x* vacancies and *m* gas atoms (subscripts *x* and *m*) are defined in the framework of the diffusion-reaction theory, in terms of the bubble radius, r_x, as follows

$$P^{j}_{x,m} = w_x D_j C_j , \tag{2}$$

$$Q^{\mathrm{v}}_{x,m} = w_x D_{\mathrm{v}} \exp\left(-E^{\mathrm{v}}_{x,m} / k_{\mathrm{B}} T\right), \tag{3}$$

$$Q^{\mathrm{g}}_{x,m} = w_x D_{\mathrm{g}} \exp\left(-E^{\mathrm{g}} / k_{\mathrm{B}} T\right) mZ / x , \tag{4}$$

where $w_x = 4\pi r_x / \Omega$, the bubble radius is found from $4\pi r_x^3 / 3 = \Omega x$ for spherical bubbles, Ω is the atomic volume: $\Omega = a^3 / n$, *a* being the lattice parameter and *n* the number of atoms in the unit cell, *n*=2 for the body-centred cubic (bcc), and *n*=4 for the face-centred cubic (fcc) lattice structures; D_j are the diffusion coefficients [m^2/s] and C_j concentrations (site fractions) of *j*-type

mobile species (j=v,i,g), $E^{\mathrm{v}}_{x,m}$ and E^{g} are the binding energies of a vacancy and a gas atom, respectively, with a gas bubble of x vacancies and m gas atoms, T is the absolute temperature, k_{B} is the Boltzmann constant, and Z is the compressibility defined in the next paragraph. The diffusion coefficients are calculated using the conventional equations through the migration energy, E^{j}_{m}, and pre-exponential factor, D_{j0}, as

$$D_j = D_{j0} \exp\left(-E^{j}_{\mathrm{m}} / k_{\mathrm{B}} T\right). \tag{5}$$

The master equation for the size distribution of interstitial loops is similar. There are two differences: first, there are no reactions with gas atoms, and, second, the dissociation reactions of interstitials from interstitial loops of any size are ignored, which is a reasonable approximation because the associated binging energies are known to be relatively high. As a result, the master equation is much simpler than for gas bubbles:

$$\frac{df^{\mathrm{iL}}_x}{dt} = G^{\mathrm{iL}}_x - P^{\mathrm{i}}_x f^{\mathrm{iL}}_x + P^{\mathrm{v}}_{x+1} f^{\mathrm{iL}}_{x+1} - P^{\mathrm{v}}_x f^{\mathrm{iL}}_x + P^{\mathrm{i}}_{x-1} f^{\mathrm{iL}}_{x-1}. \tag{6}$$

$$P^{j}_x = w_x D_j C_j, \tag{7}$$

where $w_x = 2\pi r_x / \Omega$, and the loop radius is found from $\pi r_x^2 b = \Omega x$, where b is the loop Burgers vector.

The master equation for the size distribution of vacancy loops is similar:

$$\frac{df^{\mathrm{vL}}_x}{dt} = G^{\mathrm{vL}}_x - P^{\mathrm{i}}_x f^{\mathrm{vL}}_x + P^{\mathrm{i}}_{x+1} f^{\mathrm{vL}}_{x+1} - P^{\mathrm{v}}_x f^{\mathrm{vL}}_x + P^{\mathrm{v}}_{x-1} f^{\mathrm{vL}}_{x-1}. \tag{8}$$

1.1.2. Equation of state for helium in bubbles

The compressibility factor, Z, of a gas bubble, which is needed to calculate vacancy and gas atom emission rates from a gas bubble, can defined using two alternate equations of state (EOS). The preferred EOS is the hard-sphere model by Carnahan-Starling [12]:

$$Z = \frac{1 + y + y^2 - y^3}{(1 - y)^3}, \tag{9}$$

where $y = \left(\pi\sigma^3 / 6\Omega\right)\left(m / x\right)$ is the packing fraction, and σ is the hard sphere diameter, which depends on the temperature according to the following equation:

$$\sigma = 0.3135 \times 10^{-9} \times (0.8542 - 0.03996 \times \ln(T / 9.16)) \text{ [m]}. \tag{10}$$

Here the temperature, T, is in Kelvin. For y>0.5, the Carnahan-Starling EOS was modified t

$$Z = a\ln(mb/x - c),\ \ y > 0.5, \tag{11}$$

where a=33.96855525, b=1.87 and c=0.42 [13]. An alternate EOS by Manzke and Trinkaus [14] can also be employed but is has not been tested as thoroughly as the hard-sphere equation.

The binding energy of a vacancy with a (x,m) vacancy clusters, $E^{\mathrm{v}}_{x,m}$, is defined within the well-known capillarity approximation as

$$E^{\mathrm{v}}_{x,m} = E^{\mathrm{v}}_{\mathrm{f}} - \left(2\gamma a_{\mathrm{w}} / r_x - p\right)\Omega, \tag{12}$$

where $p = \left(m/x\Omega\right)Zk_{\mathrm{B}}T$ is the gas pressure, $E^{\mathrm{v}}_{\mathrm{f}}$ is the vacancy formation energy, γ is the surface energy, and a_{w} is Wolfer's correction term [15] to the surface energy, which allows modifying the binding energy as small cluster sizes:

$$a_{\mathrm{w}} = 1 - \frac{b_{\mathrm{w}}}{4 + \dfrac{x-2}{c_{\mathrm{w}}+2}}, \tag{13}$$

where b_{w} and c_{w} are dimensionless coefficients referred to in the input as *wolfa* and *wolfn*, respectively.

1.1.3. Equations for mobile species

The concentrations, C, of mobile defects, vacancies (v), interstitials (i) and gas atoms (g) are described by the following equations (for simplicity we assume that vacancy loops are absent).

$$\frac{dC_{\mathrm{i}}}{dt} = G_{\mathrm{i}} - \mu D_{\mathrm{i}}C_{\mathrm{i}}C_{\mathrm{v}} - \left(z^{\mathrm{d}}_{\mathrm{i}}\rho_{\mathrm{d}} + z^{\mathrm{L}}_{\mathrm{i}}k^2_{\mathrm{L}} + z^{\mathrm{GB}}_{\mathrm{i}}k^2_{\mathrm{GB}} + k^2_{\mathrm{b}}\right)D_{\mathrm{i}}C_{\mathrm{i}} - 2w_1 D_{\mathrm{i}}C^2_{\mathrm{i}} + \left(P^{\mathrm{v}}f_{\mathrm{L}}\right)_{x=2} + P_{\mathrm{FP}}, \tag{14}$$

$$\begin{aligned}\frac{dC_{\mathrm{v}}}{dt} = {} & G_{\mathrm{v}} - \mu D_{\mathrm{i}}C_{\mathrm{i}}C_{\mathrm{v}} - \left(z^{\mathrm{d}}_{\mathrm{v}}\rho_{\mathrm{d}} + z^{\mathrm{L}}_{\mathrm{v}}k^2_{\mathrm{L}} + z^{\mathrm{GB}}_{\mathrm{v}}k^2_{\mathrm{GB}} + k^2_{\mathrm{b}}\right)D_{\mathrm{v}}\left(C_{\mathrm{v}} - C^{\mathrm{e}}_{\mathrm{v}}\right) \\ & - w_1 D_{\mathrm{g}}C_{\mathrm{g}}C_{\mathrm{v}} - 2w_1 D_{\mathrm{v}}C^2_{\mathrm{v}} + \left(P^{i}f\right)_{x=2,m=0} + \left(Q^{\mathrm{g}}f\right)_{x=1,m=1} + \left(Q^{\mathrm{v}}f\right)_{x=2,m=0}\end{aligned}, \tag{15}$$

$$\frac{dC_{\mathrm{g}}}{dt} = G_{\mathrm{g}} - \left(z^{\mathrm{d}}_{\mathrm{g}}\rho_{\mathrm{d}} + z^{\mathrm{GB}}_{\mathrm{g}}k^2_{\mathrm{GB}} + k^2_{\mathrm{b}}\right)D_{\mathrm{g}}C_{\mathrm{g}} - w_1 D_{\mathrm{g}}C_{\mathrm{g}}C_{\mathrm{v}} + \left(Q^{\mathrm{g}}f\right)_{x=1,m=1} + \left(Q^{\mathrm{i}}f\right)_{x=1,m=1}. \tag{16}$$

Here, μ is the recombination constant, ρ_{d} is the dislocation density, k^2_{L}, k^2_{GB} and k^2_{b} are the sink strength of interstitial loops, grain boundaries and gas bubbles, z^{d}_j are the capture efficiencies of dislocations for vacancies (j=v), interstitials (j=i) and gas atoms (j=g), respectively, z^{GB}_j are corresponding capture efficiencies for grain boundaries, G_j are the defect generation rates, and $C^{\mathrm{e}}_{\mathrm{v}}$ is the thermal-equilibrium vacancy concentration $C^{\mathrm{e}}_{\mathrm{v}} = C^{\mathrm{e}}_{\mathrm{v0}}\exp\left(-E^{\mathrm{v}}_{\mathrm{f}}/k_{\mathrm{B}}T\right)$, where $C^{\mathrm{e}}_{\mathrm{v0}}$ is the pre-exponential factor. The P_{FP} term on the RHS of equation for interstitials denote the formation of Frenkel pairs from over-pressurized bubbles.

1.1.4. Sink strengths

The sink strength of grain boundary, k^2_{GB}, of radius R_{G} equation is determined from the following equation:

$$k^2_{\mathrm{GB}} = \frac{1}{R^2_{\mathrm{G}}} \frac{3\xi^2\left(\xi\coth\xi - 1\right)}{\xi^2 - 3\left(\xi\coth\xi - 1\right)}, \tag{17}$$

where $\xi = kR_{\mathrm{G}}$, and k^2 is the total sink strength of all defects: dislocations, voids, etc. inside the grain for *j*-type defects.

The sink strength of gas bubbles/ voids, i.e. spherical sinks, is calculated as the integral over all voids, or in the grouping scheme, where Δ_x and Δ_m are the width of the groups

$$k^2_{\mathrm{b}} = \sum_m \sum_x \frac{4\pi r_x}{\Omega} f_{x,m}\Delta_x\Delta_m . \tag{18}$$

Evidently, if gas atoms are absent, i.e. void approximation is used, the size distribution of voids is one dimensional and the sum over gas atoms is absent. For planar loops, the sink strength is approximated by

$$k^2_{\mathrm{iL}} = \sum_x \frac{2\pi r_x}{\Omega} f_x^{\mathrm{iL}}(x)\Delta_x^{\mathrm{iL}} . \tag{19}$$

$$k^2_{\mathrm{vL}} = \sum_x \frac{2\pi r_x}{\Omega} f_x^{\mathrm{vL}}(x)\Delta_x^{\mathrm{vL}} . \tag{20}$$

where Δ_x^{iL} and Δ_x^{vL} are the group width.

1.1.5. Defect production rates

The point defect production rates, G_{i} and G_{v}, are equal to the NRT standard dose rate [16], G^{NRT}, corrected by the fractions of defects recombined in cascades, ε_{r}; and the fraction of defects clustered in cascades, ε_{v} ε_{i}:

$$G_{\mathrm{i}} = G^{\mathrm{NRT}}\left(1-\varepsilon_{\mathrm{r}}\right)\left(1-\varepsilon_{\mathrm{i}}\right), \tag{21}$$

$$G_{\mathrm{v}} = G^{\mathrm{NRT}}\left(1-\varepsilon_{\mathrm{r}}\right)\left(1-\varepsilon_{\mathrm{v}}\right). \tag{22}$$

The generation rate of vacancy clusters is described by

$$G_{x,m} = \begin{cases} 0, & m \neq 0 \\ Ax^{-k}, & m = 0 \end{cases}, \tag{23}$$

where *k* is a given value and *A* is found from the conservation law: $\sum_k Ax^{-k} = \varepsilon_{\mathrm{v}}$.

For interstitial clusters, vacancy loops and voids (j=iL,vL,voids) similar equations are used:

$$G_x^j = A^j x^{-k_j}. \tag{24}$$

1.1.6. Gas atom generation rates

The rate of gas generation may have a time-independent contribution, G_g, as for He production by fast neutrons, and that corresponding to He generation by thermal neutrons via ^{58}Ni(n,γ)^{59}Ni(n,α)^{56}Fe reactions. The contribution from thermal neutrons is defined by differentiation of equation (1) from reference [17]:

$$G_g^{\text{total}}(t) = G_g + \frac{\sigma_\gamma \sigma_\alpha}{\sigma_{\text{tot}} - \sigma_\varphi} F_{\text{th}} C_{^{58}\text{Ni}} \left[\exp\left(-\sigma_\gamma F_{\text{th}}\right) - \exp\left(-\sigma_{\text{tot}} F_{\text{th}}\right) \right], \tag{25}$$

where F_{th} is the thermal neutron flux, $C_{^{58}\text{Ni}}$ is the concentration of ^{58}Ni, and σ_γ , σ_α , σ_{tot} are the spectrum averaged cross-sections of (n,γ) and (n,α) reactions, and the total cross-section, respectively.

1.1.7.Generation of Frenkel pairs by over-pressurized gas bubbles

In the present model it is assumed that above certain maximum gas atom to vacancy ratio in the bubble, the bubble produces a Frenkel pair: one vacancy and one interstitial. The condition for such a reaction is thus defined by the following line in (x,m) space

$$m = g_0 + g_1 (x - 1), \tag{26}$$

where g_0 and g_1 are constants: typically g_0=5, g_1=5. These reactions are accounted by the P_{FP} term in the RHS of Eq. (1.14) for interstitials. Its value is thus calculated as

$$P_{\text{FP}} = \sum_x \left(P^g f \right)_{x, m = g_0 + g_1 (x-1)}. \tag{27}$$

The equations for the bubbles along this line contain an additional term, corresponding to the reactions:

$$(x, m) + He \rightarrow (x+1, m+1) + \text{v+i}. \tag{28}$$

Such a reaction is realised in the code within the grouping procedure developed earlier in [4-8].

1.1.8. Network dislocation evolution

The network dislocation density evolves in the present model: decreases due to mutual annihilation reactions (second term in the RHS of the following equation) and increases due to unfaulting of loops after reaching specified radius (first term in the following equation)

$$\frac{d\rho_d}{dt} = G_d - \rho_d \left(\tau_{\text{irr}}^{-1} + \tau_{\text{th}}^{-1} \right), \tag{29}$$

where the average lifetime of a dislocation for annihilation, associated with the radiation induced dislocation climb is defined as

$$\tau_{\mathrm{irr}} = \frac{b_{\mathrm{d}}}{\left(\pi\rho_{\mathrm{d}}\right)^{1/2}}\left[z_{\mathrm{i}}^{\mathrm{d}} D_{\mathrm{i}} C_{\mathrm{i}} - z_{\mathrm{v}}^{\mathrm{d}} D_{\mathrm{v}} \left(C_{\mathrm{v}} - C_{\mathrm{v}}^{\mathrm{e}}\right)\right]^{-1}, \tag{30}$$

where b_{d} is the length of the dislocation Burgers vector. The thermal contribution to this process is described by

$$\tau_{\mathrm{th}} = \left[A' \frac{2\pi^{2/3}}{\ln\left[\left(\pi\rho_{\mathrm{d}}\right)^{-1/2} / 2b_{\mathrm{d}}\right]} \frac{\Omega G D_{\mathrm{v}} C_{\mathrm{v}}^{\mathrm{e}}}{k_{\mathrm{B}} T} \rho_{\mathrm{d}} \right]^{-1}, \tag{31}$$

where A' is the modified back stress term and the generation term, see, e.g. [18]. The generation term in this equation consists of two contributions. First, the Bardeen-Herring dislocation source (see complete description in [18]) and, second, unfaulting of loops after reaching specified radius $r_{\max}$, which is defined as:

$$G_{\mathrm{d}} = \left(\frac{2\pi r_{\max}}{\Omega} \right)^2 z_{\mathrm{i}}^{\mathrm{loop}} D_{\mathrm{i}} C_{\mathrm{i}}\ , \tag{32}$$

where $z_{\mathrm{i}}^{\mathrm{loop}}$ is the capture efficiency of the loop for interstitials.

1.1.9. Correspondence between f_x and f_R

The size distributions in the (*x*,*m*) and (*R*,*m*) phase spaces are connected between each other by the relationship

$$f_{x,m} dx = f_{R,m} dR\,. \tag{33}$$

Hence, for spherical bubbles

$$f_{R,m} = f_{x,m} 4\pi R^2 / \Omega\,, \tag{34}$$

and for circular dislocation loops

$$f_{R,m} = f_{x,m} 2\pi R b / \Omega\,, \tag{35}$$

where *b* is the loop Burgers vector.

1.1.10. Grain boundary coverage

During irradiation some gas bubbles are attached to grain boundary. The grain boundary coverage, i.e. the fraction of surface occupied by bubbles, is calculated as follows:

$$f_{\mathrm{GB}} = \frac{C_{\mathrm{GB}}^{\mathrm{gas}} R_{\mathrm{G}} \left\langle R_{\mathrm{bubble}} \right\rangle^2}{3\Omega m}, \tag{36}$$

where $C_{\mathrm{GB}}^{\mathrm{gas}}$ is the total amount of gas [at^{-1}] captured by grain boundary via diffusion of single gas atoms to boundary, $\left\langle R_{\mathrm{bubble}} \right\rangle$ is the mean radius of gas bubbles in the bulk, m is the mean number of gas atoms in a bubble in the bulk. This expression is obtained assuming that the distribution of gas bubbles is random and the same in the bulk and near the grain boundary.

Swelling is calculated by integration over the size distribution of voids, as:

$$S = \sum_m \sum_x x f_{x,m} \Delta_x \Delta_m . \tag{37}$$

1.2. Geometry and boundary conditions

The integration is performed in vacancy-gas atom (x,m) space.

x: from 1 to mvv;
m: from 1 to mvb;

We assume that for certain maximum gas to vacancy ratio, the gas bubble produces a Frenkel pair: one vacancy and one interstitial. Thus, we distinguish boundaries at x=mvv (maximum value), m=mvb (maximum value for m) and $m=g_0+g_1(x-1)$, where g_0 and g_1 are constants: typically g_0=5, g_1=5. We apply the zero flux boundary conditions at these boundaries. In addition, we at 'x=1', the following reactions are forbidden:

$$(\mathrm{v},\mathrm{g}) = \mathrm{v} + \mathrm{g}; \tag{38}$$

$$(\mathrm{v},\mathrm{ng}) + \mathrm{i} = \mathrm{ng},\ \mathrm{n} > 1, \tag{39}$$

where '(v,ng)' denotes a complex of one vacancy and n gas atoms, 'i' and 'v' denote an interstitial and a vacancy, respectively. This restriction applies because of the absence of a vacancy in these complexes, since the empty space is occupied by gas atoms. Note that the reaction $(\mathrm{v},\mathrm{g}) + \mathrm{i} = \mathrm{g}$ is allowed.

1.3. Integration method

1.3.1. Grouping scheme

To reduce the number of equations, a special grouping scheme has been developed to conserve the number densities of defect clusters, as well as the total numbers of vacancies and gas atoms stored [4-8]. The main idea is to represent the size distribution inside a group by a linear function of both the number of gas atoms and number of vacancies:

$$f_{x,m} = a + b\left(x - \langle x \rangle\right) + c\left(m - \langle m \rangle\right), \tag{40}$$

where $\langle x \rangle$ and $\langle m \rangle$ are the corresponding group mean values, and *a*, *b*, *c* are constants for the group. Evidently, the coefficient *a* is equal to the mean cluster concentration in the group $\langle f_{x,m} \rangle$, while the mean values of the numbers of vacancies and gas atoms in clusters of the group are

$$\langle f_{x,m} m \rangle = a \langle m \rangle + bD_m , \tag{41}$$

$$\langle f_{x,m} x \rangle = a \langle x \rangle + bD_x , \tag{42}$$

where $D_j = \langle j^2 \rangle - \langle j \rangle^2$ are the dispersions for the group (is not to be confused with the diffusion coefficients of the mobile species). For clusters containing more than '`mvxb`' of gas atoms along `m` axis or more that '`mvxv`' of vacancies, the master equation has been reformulated in terms of *a*, *b*, *c* coefficients, which ensures the conservation laws in question.

1.3.2. Time integration

The time integration is performed using the FORTRAN subroutine package DLSODE (the Livermore Solver for Ordinary Differential Equations) written by Hindmarsh [9-11]. A solution method suitable for a stiff system of equations, with internally generated full Jacobian is employed (the description can be found in the corresponding DLSODE subroutine).

3. Typical Results of Simulations

Interim results obtained during the development of the new model have been submitted previously [2,3]. Here a few examples of recent results obtained with the completed model will be presented. A complete optimization of the input parameters using available microstructural measurements as a model calibration data set is underway. The implementation of the higher fidelity cavity evolution model has increased the number of material parameters and treating the two-dimensional helium-vacancy phase space has increased typical execution times by 10 to 100 compared to the simple initial model.

Typical results of the performance of the model are shown in Fig. 2a and b for 20% cold-worked and solution annealed materials, respectively. Results are shown for a temperature of 450°C to

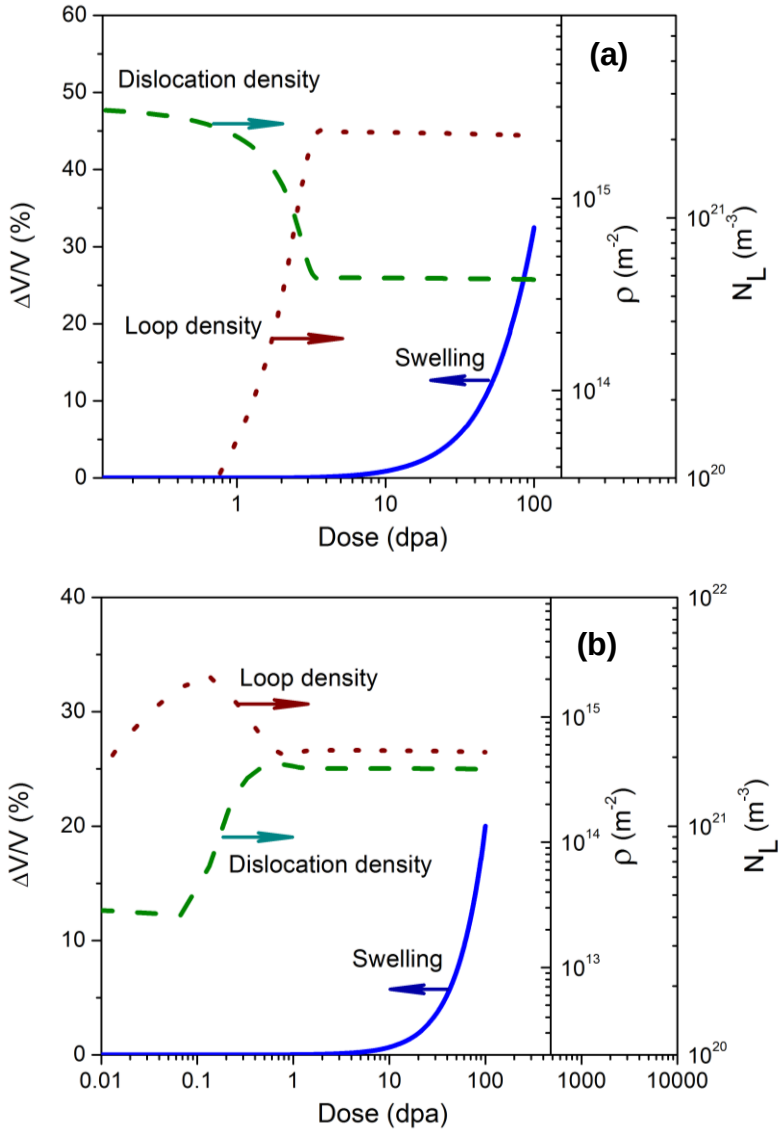

Fig. 2. Predicted dislocation evolution and void swelling under irradiation at 450°C for (a) 20% cold-worked and (b) solution annealed austenitic stainless steel.

enable more dramatic evolution to occur and to confirm that the dislocation model behaves in a manner consistent with both the original fast reactor model and available data. The primary features of note in the dislocation model are the recovery of the as-cold-worked dislocation structure and the increase in the solution annealed material due to the rapid build-up of faulted dislocation loops. These loops eventually grow large enough to unfault and become part of the dislocation network. The balance between network dislocation recovery and the creation of new network from the loops leads to a quasi-steady-state dislocation density that is nearly independent of the starting microstructure. The faulted loop density is higher at low doses in the solution annealed material but saturates at a similar level to that observed in the cold-worked material. Significant void swelling is observed following the transient in the dislocation structure.

Figures 3 and 4 provide representative results at temperatures relevant to LWR internals, T=275 and 300°C. Material and irradiation parameters are typical of LWR internal components. The predicted cavity-induced swelling is shown in Fig. 3 and the dislocation parameters are in Fig. 4.

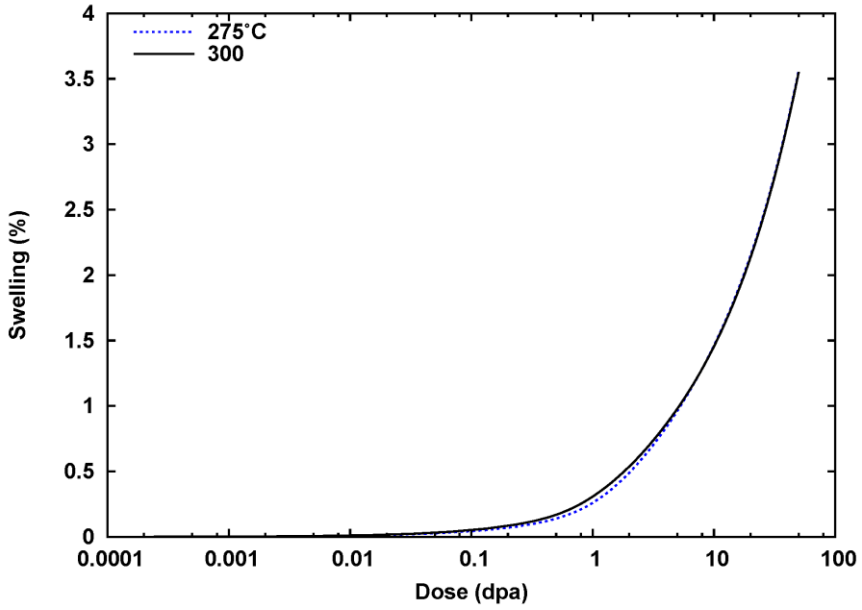

Fig. 3. Dose dependence of predicted cavity swelling at T=275 and 300°C for representative austenitic stainless steel material parameters.

Although the swelling results in Fig. 3 were obtained with a nominal, uncalibrated set of input parameters, they are consistent with the experimental observations discussed in Ref. 1 and the preliminary results obtained during model development and reported in Refs. 2 and 3. The swelling is low at both temperatures after an exposure of 50 dpa, and little difference in the dose dependence is observed between the two temperatures. The initial network dislocation density for these simulations was $5x10^{14}$ m^{-2}, which is typical of the value obtained after modest cold-working or that which evolves after several dpa (c.f. Fig. 2). Therefore, no large change is observed in the network density in Fig. 4a. During the course of the simulation a modest amount

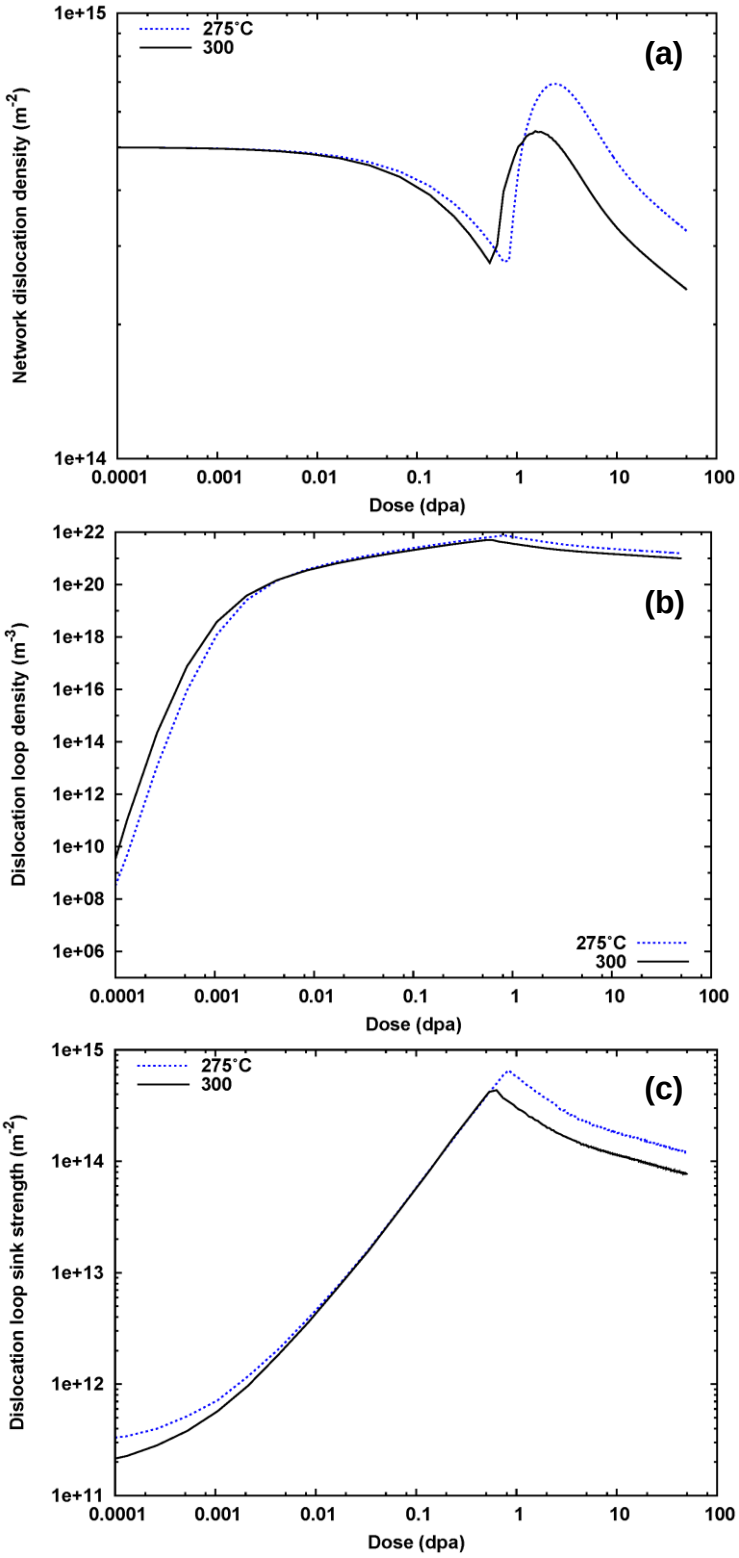

Fig. 4. Dose dependence of dislocation structure at T=275 and 300°C for representative austenitic stainless steel: (a) network dislocation density, (b) faulted dislocation loop density, and (c) faulted loop sink strength.

as the dislocation loops grow large enough to interact with the network and then unfault and add to it. The peak in the faulted dislocation loop number density observed near 1 dpa in Fig. 4b is associated with this unfaulting. The relative impact of the loops on the dislocation network can be more clearly understood by noting the magnitude of the dislocation loop sink strength in Fig. 4c.

Details of the predictions for the evolution of the dislocation components will be sensitive to a number of model parameters, including the assumed interstitial bias of both the network dislocations and the dislocation loops. The predicted swelling is also sensitive to this bias, and the bias provides a direct coupling between the evolution of the cavity and dislocation components. For example, a higher network dislocation bias would normally be expected to increase swelling. However, the higher bias will also tend to reduce the dislocation density because of increased climb and annihilation. To first order, the swelling rate is proportional to the product of the dislocation density and the bias. Therefore, depending on the relative values of the cavity and dislocation sink strengths, the net effect of a higher dislocation bias could be to either increase or decrease the swelling because of this coupling. The LWRS program is interested in a narrow temperature range; one in which microstructural evolution is relatively sluggish. In order to increase confidence in the modelling work, the model calibration effort mentioned above will encompass a wider range of temperatures

4. Implementation of the Computer Model.

The computer code is written using FORTRAN 90 and requires only a solver for the differential equations. We have employed the double precision version of the Livermore Solver for Ordinary Differential Equations (DLSODE) but others could be used. In order to reduce the execution time, it may be desirable to change to a parallel solver. A simple, potentially fail safe (but much slower) alternate Euler integration routine has also been built into the code but has not been well tested to this point. Because of its slow execution time, the Euler method would be primarily useful for debugging.

4.1 Description of Code Input

4.1. 1 An example of input file: `RIME_INPUT.dat`

```
-------------------------------------------------------------------------
INPUT for code RIME = RADIATION-INDUCED MICROSTRUCTURE EVOLUTION
-------------------------------------------------------------------------

----- Method -------------------------------------------------------------

LWRS-SS           name    -      ! Title of calculation: 12 characters
0       ONLY ZERO key     -      ! Volume =0; (Surface =1 NOT USED)
1                 keyai   -      ! Aging =0; Irradiation =1
0                 keyc    -      ! New calculation =0; Continuation =1
0                 idm     -      ! =1 check cell size
0.0               ratmax  -      ! max ratio bubble/cell size allowed
0                 keyNucl -      ! =1 - cancel nucleation: v+v and v+Gas
1.0e+10           dttt1   s      ! DLSODE max integration time-step
1.0e-3            dt0     s      ! Initial time OUT of DLSODE
1.0e+5            dttt    s      ! Max     time OUT of DLSODE
1.0               rio     -      ! Time OUT step dt=dt0+(current t)/rio
1                 nscrn   -      ! N of steps for writing to screen
1                 nremm   -      ! N of steps for writing continuation f
1                 nwrit   -      ! N of steps for writing to files
0       ONLY ZERO mfeuler -      ! EULER =1, DLSODE =0
10      *not used nround  -      ! EULER
10000   *not used nsteps  -      ! EULER n of steps dt_integ = dt/nsteps

----- Irradiation / Aging conditions -----------------------------------

1.00e+8           time    s      ! Irradiation / Aging TIME
1.00e-6           rknrt   dpa/s  ! NRT generation rate
0.67              epsr    -      ! Defect fraction recombin' in cascades
0.0               epsis   -      ! interstitial fraction in sessile clusters
0.0     *not used epsig   -      ! interstitial fraction in crowdions
0.0               epsv    -      ! Vac fraction in sessile clusters
0.0               epsw    -      ! Vac fraction in micro-voids
300.0             tc      C      ! Temperature
0.0e-5            cg0     -      ! Initial Gas-atom site fraction
3.0e+14           rod0    m-2    ! Initial dislocation density
1.0e-6            rgr     m      ! Grain radius
1.0e+6  *not used dfoil   m      ! Foil fickness for crowdions

----- He atom production  ----------------------------------------------

3.5e-13           rkhe    s-1    ! He atom generation rate
```

```
0.0e+19           Flux    n/m2/s ! Thermal neutron flux
0.0               CNi     -      ! Initial Ni58 fract' (0.68077 of all)
4.330e-28         SAlpha  m-2    ! 59Ni(n,alpha) cross section
1.630e-28         SGamma  m-2    ! 58Ni(n,gamma) ( 1 barn = 10-28 m-2 )
34.29e-28         STotal  m-2    ! 59Ni total absorption cross section

----- Material ------------------------------------------------------

4.0               type1   -      ! N at. in unit cell 2-BCC 4-FCC ?-HCP
3.58e-10          a       m      ! Lattice param': bcc Fe=2.87, fcc=3.61
3                 Nbv     -      ! Loop Burgers V: 1-S3/2; 2-0.5; 3-1/S3
4.05              gamma0  J/m2   ! Surface energy defined as
0.5               gama    -      ! -- (gama*gamma0-gamtc*tc)/1.6e-19
0.00175           gamtc   J/m2/C ! -- which is in eV
1.6               evf     eV     ! Vacancy formation energy
1.4               evm     eV     ! Vacancy migration energy
0.85              eim     eV     ! Interstitial migration energy
0.3     *not used egm     eV     ! Crowdion migration energy
0.3               ehm     eV     ! Gas-atom migration energy
1.0               cve0    -      ! Pre-exp for vacancy  formation
8.0e-5            c0v     m2/s   ! Pre-exp for vacancy  migration
8.0e-6            c0i     m2/s   ! Pre-exp for interstitial migration
1.0e-6  *not used c0g     m2/s   ! Pre-exp for crowdion migration
5.0e-8            dh0     m2/s   ! Pre-exp for gas atom migration
0.0e+0            Sdisl   m-3    ! Bardeen-Herring disl' source density
0.0               Aprime  -      ! Modified back stress term, 0.05 in [18]

----- Reaction cross-sections ---------------------------------------

1.25              zicl    -      ! Loop capture effic' for interstitials
1.25              zi      -      ! Disl' capture effic' for interstitials
1.0               zv      -      ! Disl' capture effic' for vacancies
0.0               zgd     -      ! Disl' capture effic' for gas atoms
1.0               zig      -     ! GB    capture effic' for interstitials
1.0               zvg     -      ! GB    capture effic' for vacancies
0.0               zgg     -      ! GB    capture effic' for Gas atoms
1.0               rava    -      ! fraction of sites for gas at at disl'
2.25              edge    eV     ! emission energy for gas at from disl'
2.0e+21           rec     m2/s   ! Recombination constant
1.0     *not used rkk     -      ! v+crow =1-pure 1D; =0-preferential
1       ONLY ONE  keybb   -      ! EOS:1-Stoller [13];2-Carnahan-Starling
                                   [12];3-Manzke-Trinkaus [14]
0.2e-9            sigma   -      ! Sigma for Carnahan-Starling EOS
2.1               wolfa   -      ! Wolfer correction [15]; see Eqn. (13)
1.0               wolfn   -      ! Wolfer correction
10000             nevf    -      ! i>nevf then Ev_binding=evf
1                 keyart  -      ! =1 include punching of i from bubbles
2.3               eeg     eV     ! Gas atom-bubble binging energy
0.5e-9  *not used rro     m      ! Disloc'  capture radius for crowdions
3.0e-10 *not used hilg    m      ! interstitial loop capture radius for
                                   crowdions
3.0e-10 *not used hvlg    m      ! Vac loop capture radius for crowdions

----- Bubbles: vacancies --------------------------------------------

10                mwm     -      ! Max size for generation ( < mvxv )
1.0               pnw     -      ! Exponent: gener rate ~ i**(-pnw)
10                mvxv    -      ! i > mvxv: groups
0.12              drvv    nm     ! dr or dr/r for groups see below
```

```
2                igrvac  -       ! =1 - dr; =2 - dr/r for above choice
1                ifac    -       ! Factor: increase size of last group
44               nvv     -       ! Min i visible

----- Bubbles: gas atoms ---------------------------------------------

10               mvxb    -       ! j > mvxb: groups
0.12             drvb    nm      ! dr or dr/r for groups see below
2                igrgas  -       ! =1 - dr; =2 - dr/r for above choice
50               nvb     -       ! Min j visible
4.5              g00     -       ! Definition for upper boundary
5.0              g11     -       ! for Gas atom area: g < g00+g11*(x-1)
80               iimax   -       ! N of vac points to write E_bin & emis
60               ijmax   -       ! N of gas points to write E_bin & emis

----- Interstitial loops ---------------------------------------------

10               mim     -       ! Max size for generation ( < mixl )
1.0              pni     -       ! Exponent: gener rate ~ i**(-pni)
20               mixl    -       ! i > mixl:  groups
6.0e-10          dri     m       ! dr in groups
20               nli     -       ! Min i visible

----- Vacancy loops --------------------------------------------------

9                mvm     -       ! Max size for generation ( < mvxl )
1.0              pnv     -       ! Exponent: gener rate ~ i**(-pnv)
10               mvxl    -       ! i > mvxl:  groups
1.0e-10          drvl    m       ! dr in groups
20               nlv     -       ! Min i visible

----- Hardening ------------------------------------------------------

80.0e+09         g       n/m2    ! Shear modulus
240.0            sigma0  MPa     ! Initial stress yield
135.0            hard0   Vikers  ! Initial hardness
2.0              fsht    -       ! Shmidt-Taylor factor
2.7              sihard  Vikers  ! Sigma to hardness coefficient
1.0              ali     -       ! Dimensionless coefficients
1.0              alv     -       ! --for estimation of hardening
1.0              alc     -       ! --due to i and v loops and cavities

------------------------------------------------------------------------
-END of INPUT DATA-----------------------------------------------------
------------------------------------------------------------------------
```

4.2. Line-by-line description of the input file

Free format is used. The input parameters are defined by `implicit real*8 (a-h,o-z)` and integer for (i-n). General format of the input for a parameter '`name`' of dimensions [units] with the value '`value`' is

```
value              name     units      ! Description
```

`Units='-'` indicates a dimensionless parameter.

4.2.1. Headline

```
------------------------------------------------------------------------
INPUT for code RIME = RADIATION-INDUCED MICROSTRUCTURE EVOLUTION
```

```
-------------------------------------------------------------------------
```

4.2.2. Group of parameters defining the problem in general

```
----- Method -------------------------------------------------------
```

4.2.3. Title of calculation

```
LWRS-SS          name     -       ! Title of calculation: 12 characters
```

A short (character*12) description of the problem to appear in the first line of the screen output.

4.2.4. Volume or surface calculations

```
0        ONLY ZERO key      -       ! Volume =0; (Surface =1 NOT USED)
```

This parameter must be equal to 0 (volume calculation) in this version of the code.

4.2.5. Irradiation or aging

```
1               keyai    -          ! Aging =0; Irradiation =1
```

Parameter defining whether the calculation is for irradiation (‘keyai=1’) or aging (‘keyai=0’) conditions. Note that for aging there is no need to put the irradiation parameters: the defect production rate, He generation rate and thermal neutron flux to zero: all these will be done automatically inside the code.

4.2.6. New calculation or continuation of old calculation

```
0                  keyc     -       ! New calculation =0; Continuation =1
```

Parameter defining whether the calculation is new (‘keyc=0’) or old (‘keyc=1’). The following table explains the use of this parameters for different calculations.

Aim of calculation	Parameter	Files required
Start new irradiation calculation	keyc=0	None
Start new aging calculation	keyc=0	zz_irr_ct.dat
Continue aging calculation to a longer time	keyc=1	zz_age_ct.dat
Continue irradiation calculation to a longer dose	keyc=1	zz_irr_ct.dat

where zz_irr_ct.dat is a file created during a run of irradiation case; and zz_age_ct.dat is a file created during a run of aging case.

4.2.7. On-the-fly control of calculation cell size

```
0               idm      -          ! =1 check simulation cell size
1.e-3           ratmax   -          ! max ratio bubble/cell size allowed
```

Two parameters for controlling the size of calculation cell: ‘idm’ is an on-off switch of the function. If ‘idm=0’ the value of ‘ratmax’ is not used. If ‘idm=1’, the code stops when the ratio of the mean bubble radius (calculated starting from first visible size ‘nvv’) to the maximum radius, corresponding to the maximum value of the ‘mvv-1’ group, becomes higher than the value ‘ratmax’. In this case, the code writes the following message on screen:

```
The code stopped because the ratio of the mean bubble radius = 4.479E-01
[nm] and the maximum bubble radius radvm  = 5.786E-01 [nm] is greater than
ratmax = 5.000E-01
Increase simulation cell (mvv=  20) and continue.
```

4.2.8. Cancelling nucleation

```
0                keyNucl -      ! =1 - cancel nucleation: v+v and v+Gas
```

Switch for canceling nucleation of gas bubbles/voids, used for some special purposes.

4.2.9. Time steps

```
1.0e+10       dttt1  s         ! DLSODE max integration time step
1.0e-3        dt0    s         ! Initial time OUT of DLSODE
1.0e+5        dttt   s         ! Max     time OUT of DLSODE
1.0           rio    -         ! Time OUT step dt=dt0+(curr t)/rio
```

The ‘dttt1’ is the maximum time step of the DLSODE integration and is the only DLSODE parameter in the input file (the others being in the ‘module USER_mod’). The other three time parameters define sequence of times when the code comes out of the DLSODE to record intermediate results. The next such time is defined by the time increment using the equation dt=dt0+(curr t)/rio, where ‘curr t’ is the current time in seconds. For ‘dt’ exceeding ‘dttt’, ‘dt=dttt’ is used instead.

4.2.10. Frequency of writing files

```
1             nscrn   -         ! N of steps for writing to screen
1             nremm   -         ! N of steps for writing continuation f
1             nwrit   -         ! N of steps for writing to files
```

Parameters defining frequency of writing results to screen (‘nscreen’), writing a binary file for continuation (‘nremm’) and writing intermediate results to text files (‘nwrit’). These are in terms of the number of steps ‘dt’. The value ‘1’ corresponds to the most frequent writing: each time the code goes out of the DLSODE, corresponding data are recorded.

4.2.11. Group of parameters for Euler integration method

```
0       ONLY ZERO mfeuler -      ! EULER =1, DLSODE =0
10      *not used nround  -      ! EULER
10000   *not used nsteps  -      ! EULER n of steps dt_integ = dt/nsteps
```

Not used in the current version of the code.

4.2.12. Group of parameters defining irradiation or aging conditions

```
----- Irradiation / Aging conditions ----------------------------------
```

4.2.13. Physical time

```
2.0e+4          time    s          ! Irradiation / Aging TIME
```

Time in seconds. The code stops when this value is reached.

4.2.14. Description of defects production in cascades

```
1.00e-6       rknrt   dpa/s  ! NRT generation rate
0.67          epsr    -      ! Defect fraction recombin' in cascades
0.0           epsis   -      ! interstitial fraction in sessile clusters
0.0 *not used epsig   -       ! interstitial fraction in crowdions
0.0           epsv    -      ! Vac fraction in sessile clusters
0.0           epsw    -      ! Vac fraction in micro-voids
```

The NRT standard [16] damage rate [dpa/s] (there is no need to set this parameter to zero in the case of aging calculations: the code will do this automatically), and parameters defining various fractions of defects produced in a cascade: fraction of defects recombined with respect to the NRT standard value; interstitial fraction produced in the form of sessile clusters, vacancy fractions in sessile clusters (small dislocation loops) and spherical micro-voids.

4.2.15.Irradiation conditions and materials microstructure

```
300.0             tc      C      ! Temperature
0.0e-5            cg0     -      ! Initial Gas-atom site fraction
3.0e+14           rod0    m-2    ! Initial dislocation density
1.0e-6            rgr     m      ! Grain radius
1.0e+6  *not used dfoil   m      ! Foil thickness for crowdions
```

Temperature (degree C), initial concentration (site fraction) of gas atom assumed to be randomly distributed over the volume, initial dislocation density, and grain radius.

4.2.16. Gas-atom production

```
----- He atom production  ---------------------------------------------

2.5e-13      rkhe    s-1       ! He-generation rate
0.0e+19      Flux    n/m2/s    ! Thermal neutron flux
0.68077      CNi     -         ! Total Ni site fraction
5.75e-28     SAlpha  m-2       ! 59Ni(n,alpha) cross section
2.24e-28     SGamma  m-2       ! 58Ni(n,gamma) cross section
45.58e-28    STotal  m-2       ! 59Ni total absorption cross section
```

He-atom generation rate [s^{-1}] by fast and thermal neutrons. The fast neutron contribution (rkhe) is constant in time. The contribution from thermal neutrons is defined by differentiation of equation (1) from reference [14]. The following are parameters defining He-atom production by $^{58}Ni(n,\gamma)^{59}Ni(n,\alpha)^{56}Fe$ reactions during irradiation. 'Flux' is the thermal neutron flux in [n m^{-2} s^{-1}], and 'CNi' is the initial atomic fraction of Ni atoms. The spectrum-averaged cross-sections of (n, α) ('SAlpha') [m^2], (n,γ) ('SGamma') [m^2] reactions and for total absorption ('STotal') [m^2] are taken from table III in [14]. There is no need to set any of these parameters to zero in the case of aging calculations: the code will do this automatically.

4.2.17. Material properties

```
----- Material ------------------------------------------------------

4.0              type1   -       ! N at. in unit cell 2-BCC 4-FCC ?-HCP
3.58e-10         a       m       ! Lattice param': bcc Fe=2.87, fcc=3.61
3                Nbv     -       ! Loop Burgers V: 1-S3/2; 2-0.5; 3-1/S3
4.05             gamma0  J/m2    ! Surface energy defined as
0.5              gama    -       ! -- (gama*gamma0-gamtc*tc)/1.6e-19
0.00175          gamtc   J/m2/C  ! -- which is in eV
1.6              evf     eV      ! Vacancy  formation energy
1.4              evm     eV      ! Vacancy  migration energy
0.85             eim     eV      ! interstitial migration energy
0.3    *not used egm     eV      ! Crowdion migration energy
0.3              ehm     eV      ! Gas-atom migration energy
1.0              cve0    -       ! Pre-exp for vacancy  formation
8.0e-5           c0v     m2/s    ! Pre-exp for vacancy  migration
8.0e-6           c0i     m2/s    ! Pre-exp for interstitial migration
1.0e-6 *not used c0g     m2/s    ! Pre-exp for crowdion migration
5.0e-8           dh0     m2/s    ! Pre-exp for gas atom migration
0.0e+0           Sdisl   m-3     ! Bardeen-Herring disl' source density
0.0              Aprime  -       ! Modified back stress term, 0.05 in [15]
```

Material parameters as defined on the right-hand sides. The parameter '`type1`' must be either 2 or 4 (number of atoms in unit cell), for the bcc and fcc crystal lattice, respectively. The hcp lattice anisotropy is not included into the code. The length of the dislocation loop Burgers vector is chosen from the list, where Nbv=1 corresponds to (√3/2)a as for ½ <111> loop in bcc metals, Nbv=2 to (1/2)a, as for ½ <100> in bcc metals, and Nbv=3 to (1/√3)a, as for faulted loop in fcc crystal lattice. The next three parameters define temperature dependence of the surface energy, which is necessary in the code to calculate the binding energies of vacancies with vacancy defects, such as voids, vacancy loops and gas bubbles. The following parameters define diffusion coefficients of corresponding species indicated on the right hand side: single vacancies, interstitials and gas (e.g. He) atoms. The Bardeen-Herring source density for dislocations and the modified back stress term define the behavior of dislocations.

4.2.18. Reaction cross-sections

```
----- Reaction cross-sections ---------------------------------------
```

```
1.25              zicl    -       ! Loops capture effic' for interstitials
1.25              zi      -       ! Disl' capture effic' for interstitials
1.0               zv      -       ! Disl' capture effic' for vacancies
0.0               zgd     -       ! Disl' capture effic' for gas atoms
1.0               zig      -      ! GB    capture effic' for interstitials
1.0               zvg     -       ! GB    capture effic' for vacancies
0.0               zgg     -       ! GB    capture effic' for Gas atoms
1.0               rava    -       ! fraction of sites for gas at at disl'
2.25              edge    eV      ! emission energy for gas at from disl'
2.0e+21           rec     m2/s    ! Recombination constant
1.0     *not used rkk     -       ! v+crow =1-pure 1D; =0-preferential
1       ONLY ONE  keybb   -       ! EOS:1-Stoller [13]; 2-Carnahan-Starling
                                    [12];3-Manzke-Trinkaus [14]
0.2e-9            sigma   -       ! Sigma for Carnahan-Starling EOS
2.1               wolfa   -       ! Wolfer correction; see Eqn. (15)
1.0               wolfn   -       ! Wolfer correction
10000             nevf    -       ! i>nevf then Ev_binding=evf
1                 keyart  -       ! =1 include punching of i from bubbles
2.3               eeg     eV      ! Gas atom-bubble binging energy
0.5e-9  *not used rro     m       ! Disloc'  capture radius for crowdions
3.0e-10 *not used hilg    m       ! interstitial loop capture radius for
                                    crowdions
3.0e-10 *not used hvlg    m       ! Vac loop capture radius for crowdions
```

A group of parameters defining reaction cross-sections. ‘zicl’ is the capture efficiency of interstitial loops for dislocations: it may be different from the corresponding dislocation efficiency due to difference in the Burgers vector orientation and length. ‘zi’ and ‘zv’ are the dislocation capture efficiencies. ‘zgd’ is the corresponding parameter for gas atoms. ‘zig’, ‘zvg’, ‘zgg’ are similar capture efficiencies of grain boundaries for interstitials, vacancies and gas atoms respectively. ‘rec’ is the recombination constant [m^{-2}]. Parameter ‘sigma’ [m] is the hard-sphere diameter in the Carnahan-Starling equation of state (EOS) [12]. ‘eeg’ is the binding energy of a gas atom with a bubble [eV]. Wolfa and wolfn are parameters defining Wolfer’s correction term [15] to the surface energy in the vacancy-bubble/void binding energy, see Eqn. (13). The parameter keyart allows switching off the punching of Frenkel pair by highly pressurized bubbles.

4.2.16. Gas bubble size distribution: vacancy part

```
----- Bubbles: vacancies ---------------------------------------------

3                 mwm     -         ! Max size for generation ( < mvxv )
1.0               pnw     -         ! Exponent: gener rate ~ i**(-pnw)
15                mvxv    -         ! i > mvxv: groups
0.1               drvv    nm-       ! dr or dr/r for groups see below
2                 igrvac  -         ! =1 - dr; =2 - dr/r for above choice
1                 ifac    -         ! Factor: increase size of last group
20                nvv     -         ! Min i visible
```

Parameters determining the vacancy axis of the bubble size distribution. Small clusters containing less than ‘mwm’ vacancies and zero gas atoms may be produced in cascades if the fraction of vacancies in such clusters defined by ‘epsw’ is nonzero. The clusters of *i*

vacancies are produced with the rates proportional to i^{-pnw}, where '`pnw`' is a dimensionless parameter. The size distribution is described by groups above the size '`mvxv`'. The group width is increased proportionally to constant radius increment '`drvv`' [nm] if '`igrvac=1`', or proportionally to '`drvv*r`', if '`igrvac=2`', where '`drvv`' is now dimensionless parameter and '`r`' is the bubble radius. '`ifac`' is the factor by which the width of the last group is increased. The clusters containing bigger than or equal to '`nvv`' vacancies are considered to be visible in microscope.

4.2.17. Gas bubble size distribution: gas atom part

```
----- Bubbles: gas atoms ------------------------------------------------

15              mvxb    -       ! j > mvxb: groups
0.1             drvb  nm-       ! dr or dr/r for groups see below
2               igrgas  -       ! =1 - dr; =2 - dr/r for above choice
50              nvb     -       ! Min j visible
4.5             g00     -       ! Definition for upper boundary
5.0             g11     -       ! for Gas atom area: g < g00+g11*(x-1)
100             iimax   -       ! N of vac points to write E_bin & emis
100             ijmax   -       ! N of gas points to write E_bin & emis
```

Description of the gas-atom axis for the gas bubble size distribution is constructed in analogy with that along the vacancy axis, as if gas atoms were on substitution sites. The groups started above the size '`mvxb`'. The group width is increased proportionally to a constant radius increment '`drvb`' [nm] if '`igrgas=1`', or if '`igrvgas=2`', proportionally to '`drvb*r`', where '`drvv`' is dimensionless parameter and '`r`' is the (fictitious) radius. '`g00`' and '`g11`' define the line `ng=g00+g11*(x-1)`, where `ng` is the number of gas atoms, and `x` is the number of vacancies, above which the size distribution is assumed to be zero and bubbles capturing gas atoms produce a Frenkel pair. Along this line, zero flux boundary conditions are applied. iimax and ijmax define the number of points for writing binding energy and emission rates files.

4.2.18. Interstitial and vacancy loops

Description of interstitial and vacancy loops is analogous to that for bubbles and does not need explanation.

```
----- Interstitial loops ------------------------------------------------

10                mim     -       ! Max size for generation ( < mixl )
1.0               pni     -       ! Exponent: gener rate ~ i**(-pni)
20                mixl    -       ! i > mixl:  groups
6.0d-10           dri     m       ! dr in groups
20                nli     -       ! Min i visible

----- Vacancy loops -----------------------------------------------------

9                 mvm     -       ! Max size for generation ( < mvxl )
1.0               pnv     -       ! Exponent: gener rate ~ i**(-pnv)
```

```
10                mvxl    -       ! i > mvxl:  groups
1.0d-10           drvl    m       ! dr in groups
20                nlv     -       ! Min i visible
```

4.2.19. Gas bubble size distribution: gas atom part

```
----- Hardening ------------------------------------------------------

80.0d+09          g       n/m2    ! Shear modulus
240.0             sigma0  MPa     ! Initial stress yield
135.0             hard0   Vikers  ! Initial hardness
2.0               fsht    -       ! Shmidt-Taylor factor
2.7               sihard  Vikers  ! Sigma to hardness coefficient
1.0               ali     -       ! Dimensionless coefficients
1.0               alv     -       ! --for estimation of hardening
1.0               alc     -       ! --due to i and v loops and cavities
```

These parameters are for the description of hardness increase due to accumulation of various defects in irradiated sample.

```
-----------------------------------------------------------------------
-END of INPUT DATA-----------------------------------------------------
-----------------------------------------------------------------------
```

This is the end of input file.

4.3. Additional input in '`module USER_mod`'

The following lines in the module USER_mod, which is most important to a user are indicated by the word FLAG.

```
c                                ERROR TOLERANCES (convergence criteria)
c
      parameter ( rtol = 1.d-3 , atsia= 1.d-14, atvac= 1.d-11 )  ! FLAG
      parameter ( ntol = 10    , atcro= 1.d-13, atgas= 1.d-18 )  ! FLAG
      parameter ( atbub= 1.d-20, atlps= 1.d-16, atdis= 1.d+9  )  ! FLAG
c
c                                                              KEYS & SIZE
c
c                                           !!! iCrow must be =0
      parameter ( iHe  = 0, iVac  = 1, iInt  = 1, iCrow= 0 )     ! FLAG
      parameter ( iVoid= 1, iVloop= 0, iIloop= 0, iDisl= 0 )     ! FLAG
      parameter ( mvv= 20, mvb= 20, mil= 53, mvl= 8 )            ! FLAG
```

These are the main parameters for a user, and are defined as follows.

rtol	- relative tolerance for all calculated values;
atsia	- absolute tolerance for the concentration of interstitials;
atvac	- absolute tolerance for the concentration of vacancies;
atcro	- absolute tolerance for the concentration of crowdions;
atgas	- absolute tolerance for the concentration of gas atoms;
atbub	- absolute tolerance for the size distribution of gas bubbles/voids;
atlps	- absolute tolerance for the size distribution of loops;
atdis	- absolute tolerance for the dislocation density;
ntol	- absolute tolerance for the gradients of size distribution inside a group, which is calculated as absolute tolerance for corresponding size distribution divided by ntol.

The total absolute tolerance of a value is calculated as the sum of corresponding absolute tolerance and rtol*abs(value), where 'value' is the computed value.

The following switches to include or exclude a defect from calculation are used:

iHe	- switch for gas atoms:	0- excluded; 1- included;
iVac	- switch for single vacancies:	0- excluded; 1- included;
iInt	- switch for single interstitials:	0- excluded; 1- included;
iCrow	- switch for crowdions:	0- excluded in this version of the code;
iVoid	- switch for voids:	0- excluded; 1- included;
iVloop	- switch for vacancy loops:	0- excluded; 1- included;
iIloop	- switch for interstitial loops:	0- excluded; 1- included;
iDisl	- switch for dislocation density:	0- constant; 1- evolving density.

The array dimensions of vacancy grid and gas-atom grid for two-dimensional SD of gas bubbles are defined as follows:

mvv	- array size for vacancy grid for gas bubbles/voids;

mvb - array size for gas atom axis for gas bubbles.

Note that the first value is also used for a one-dimensional size distribution of voids without gas atoms. Voids (no gas) correspond to iVoid=1 and iHe=0, while gas bubbles to iVoid=1 and iHe=1.

4.4 Description of Code Output

Output from the code comprises a series of pre-named output files that are written to the local disk space as discussed in Section 3.2 below. In addition, there is a stream of intermediate output sent to the default output device on unit 6, which is usually the display on a linux system. This 'screen' output can be useful to monitor the progression of a job, and it can redirected to a file more convenient examination.

4.4.1. Output to screen

An example of the output to screen is given below. The lines are left-numbered, and these numbers are used below for the line by line explanation.

4.4.1. Example of the head at the beginning of calculations

```
01 gamma = 1.150E+00 [J/m**2]  7.188E+18 [eV/m**2]
02 E_binding_v-(v2g1) = 1.243E+00 eV
03 Wolfer correction  = 4.750E-01
04 Start new calculation
05 Volume
06 Irradiation
07 Time0= 0.00E+00 neq= 2805 rtol= 1.000E-03
08 Burgers vector N=           3  =    2.0669139636988603E-010
09 TimeF= 1.00E+04
10 iVac=1 iInt=1 iCrow=0 iHe=1 iVoid=1 iDisl=1 iVloop=0 iIloop=1
11 Vac groups from= 10 max=  30 id=   54
12 Gas groups from= 10 max=  30
13 Max R_void=   2.2388443099067721      nm
14 tgdi=   0.0000000000000000
```

4.4.2. Line by line explanation of the head of calculations

```
01 gamma = 1.150E+00 [J/m**2]  7.188E+18 [eV/m**2]
```

- Surface energy in two different units for calculating vacancy binding energy with vacancy type defects: voids, gas bubbles and vacancy loops using capillarity theory with Wolfer's correction term [15] for small vacancy clusters.

```
02 E_binding_v-(v2g1) = 1.243E+00 eV
```

- Binding energy of a vacancy with a defect complex containing two vacancies and one gas atom [eV]. It is used for fitting this value by using different values for Wolfer's correction parameters and surface energy.

```
03 Wolfer correction = 4.750E-01
```

- This is the Wolfer correction factor.

```
04 Start new calculation
05 Volume
06 Irradiation
```

- These three lines define calculation as new (not continuation of old) bulk irradiation.

```
 07 Time0= 0.00E+00 neq= 2805 rtol= 1.000E-03
```

- Initial time [s], total number of equations and relative tolerance for all calculated values.

```
 08 Burgers vector N=       3  =    2.0669139636988603E-010
```

- Burgers vector index and length in [m].

```
 09 TimeF= 1.00E+04
```

- Final time [s] until which the calculation will proceed.

```
 10 iVac=1 iInt=1 iCrow=0 iHe=1 iVoid=1 iDisl=1 iVloop=0 iIloop=1
```

- List of defects included into and excluded from the calculation. In the example provided, single vacancies and interstitials are included, but crowdions not; gas (He) atoms and dislocations (their evolution, otherwise dislocation density will be constant) are included, but vacancy loops are not. Interstitial loops are included.

```
 11 Vac groups from= 10 max=  30 id=   54
 12 Gas groups from= 10 max=  30
 13 Max R_void=   2.2388443099067721      nm
```

- These lines characterize gas bubble description by stating that single size description is used for clusters smaller than 10 and groups of cluster size for clusters >= 11 vacancies. The number of groups including singles is 30 and the maximum array size in the code is 54. The description of gas grid is defined the same way. The maximum radius of void is given in [nm].

```
 14 tgdi=   0.0000000000000000
```

- The gas atoms are stored at dislocations [at^{-1}]: zero at the beginning of new calculations it may be non-zero if calculation is continued.

4.4.3. Example of the repetitive part for different irradiation/aging times

```
 01 OR-RIME.V2: LWRS-SS      ISTATE= 2 mf=22
 02 DLSODE timestep = 2.075E-04 Order= 3
 03 T   = 500.0    rod= 3.0E+14 Rg  = 1.0E-06
 04 GHe = 3.50E-13 CNi= 0.0E+00 Flux= 0.000E+00
 05 GNRT= 1.00E-06 Di = 2.3E-11 DCi = 7.445E-22
 06 DNRT= 1.00E-09 Dv = 6.0E-14 DCv = 1.943E-23
 07 Time= 1.00E-03 Dh = 5.5E-10 R/S = 1.937E-03
 08 dt  = 1.00E-03 Cve= 3.7E-11 RWZ = 2.993E+02
 09 Max size  il vl v/g         53          8   30/   30 dmx= 2.239E+00
 10 <R> from 2    [nm ]      0.188      0.000      0.176 Ci = 3.241E-11
 11  N  from 2    [m-3]  3.244E+14  0.000E+00  7.902E+13 Cv = 3.262E-10
 12 <R> from n    [nm ]      0.594      0.000      0.529 Cg = 1.000E-35
 13  N  from n    [m-3]  1.904E-67  0.000E+00  9.558E-69 CHe= 3.462E-16
 14  N  at bound  [m-3]  9.701-256  0.000E+00 -2.492-179 <m>= 4.176E-03
 15  n  visible   [---]         20         20         44 sdt= 1.809E-04
 16  SS for 1d Gl [m-2]  0.000E+00  0.000E+00  0.000E+00 sth= 1.928E-10
 17  SS for 3d-i  [m-2]  1.201E+10  0.000E+00  2.892E+05 v+g= 7.840E+10
 18  SS for 3d-v  [m-2]  5.577E+05  0.000E+00  3.377E+05 v+v= 3.089E+11
```

```
19  Emission ivv [m-2]  1.207E-17  0.000E+00  1.208E-15 rod= 3.000E+14
20  N*<x>        [---]  7.442E-15  0.000E+00  1.809E-13 Sge= 3.785E-18
21  Critical cl. [---]                    0          0 GBH= 0.000E+00
22  Y fractions  [---]  6.767E-01  0.000E+00  3.233E-01
23  Y= 6.03E-03  [MPa]  dS= 1.207E-02 S= 2.400E+02
24               [Vic]  dH= 4.469E-03 H= 1.350E+02
25  Critical nucleus    rcr= 0.000E+00 xcr= 0.000E+00 mcr= 0.000E+00
26 L1D= 1.41E-20 gv/= 4.45E+02 ssGB= 1.00E-03 sbi= 2.86E+05 sbv= 2.86E+05
27 Ggb= 0.00E+00 Gbc= 1.50E-14 Sw0 = 1.81E-15 SwR= 1.81E-15 dVV=-1.11E-16
28 Gdi= 1.17-316 Gbe= 7.37E-19 Sv0 = 0.00E+00 Sg0= 3.78E-18 dGG= 0.00E+00
29 Gge= 3.50E-16 Gco= 1.07E-10 Si0 = 7.44E-15
30 GB sink strength for ivg=  6.735E+13  6.141E+13  0.000E+00
```

4.4.4. Line by line explanation of the repetitive part

```
01 OR-RIME.V0: LWRS-SS      ISTATE= 2 mf=22
```

- Name of the version of the code and a short identification of the task defined in the INPUT file. ISTATE characterizes the state of integration by the DLSODE: 1 - first call, 2 - normal, continue with no parameters changed, 3 - continue with changed parameters, including: mf, neq, rtol, etc. Read more in the DLSODE subroutine. `mf` is the DLSODE parameter for integration method (see DLSODE), mf=22 is for stiff method with internally generated Jacobian.

```
02 DLSODE timestep = 2.075E-04 Order= 3
```

- The DLSODE maximum time-step of integration and integration order.

```
03 T   = 500.0    rod= 3.0E+14 Rg  = 1.0E-06
```

-Temperature [^{o}C], the dislocation density [m^{-2}], and the grain radius [m].

```
04 GHe = 3.50E-13 CNi= 0.0E+00 Flux= 0.000E+00
```

- The gas (e.g. He) atom generation rate [atom/s], Ni concentration [at^{-1}], the thermal neutron flux [$n/m^2/s$]: all these parameters are needed to calculate gas atom production rate.

```
05 GNRT= 1.00E-06 Di = 2.3E-11 DCi = 7.445E-22
```

- The NRT production rate of Frenkel pairs [dpa/s], the diffusion coefficient of interstitials (D_i) [m^2/s], and the product D_i*C_i [m^2/s], where C_i is the interstitial concentration (site fraction) [at^{-1}].

```
06 DNRT= 1.00E-09 Dv = 6.0E-14 DCv = 1.943E-23
```

- Current NRT irradiation dose [dpa], the diffusion coefficient of vacancies (D_v) [m^2/s] and the product of D_v*C_v [m^2/s] , where C_v is the vacancy concentration (site fraction) [at^{-1}].

```
07 Time= 1.00E-03 Dh = 5.5E-10 R/S = 1.937E-03
```

- Current (elapsed) time [s], the gas (e.g. He) atom diffusion coefficient [m^2/s], and the ratio of point defect recombination rate and the rate of point defects loss of defects at sinks.

```
08 dt  = 1.00E-03 Cve= 3.7E-11 RWZ = 2.993E+02
```

- The increment of time since the previous output [s], the thermal equilibrium vacancy concentration [at^{-1}], the Wigner-Seitz cell for voids/gas bubbles [nm].

```
 09 Max size  il vl v/g         53          8   30/   30 dmx= 2.239E+00
```

- In this example, the numbers 53 and 8 are the array size for the description of interstitial and vacancy loops stored. 30/30 are the array size for the vacancy and gas grids in the description of gas bubbles, and dmx is the maximum bubble radius (corresponding to the array index `mvv`-1) [nm].

```
 10 <R> from 2    [nm ]      0.188      0.000      0.176 Ci = 3.241E-11
```

- The mean radius of interstitial and vacancy loops, and void/gas bubbles [nm], and the concentration of interstitials [at^{-1}].

```
 11  N  from 2    [m-3]  3.244E+14  0.000E+00  7.902E+13 Cv = 3.262E-10
```

- The number density of the same defects [m^{-3}], and the vacancy concentration [at^{-1}].

```
 12 <R> from n    [nm ]      0.594      0.000      0.529 Cg = 1.000E-35
```

- The mean radius of visible defects [nm] (see definition two lines below), and the concentration of crowdions [at^{-1}].

```
 13  N  from n    [m-3]  1.904E-67  0.000E+00  9.558E-69 CHe= 3.462E-16
```

- The number density of visible defects [m^{-3}], and the gas atom concentration [at^{-1}].

```
 14  N  at bound  [m-3]  9.701-256  0.000E+00 -2.492-179 <m>= 4.176E-03
```

- The density of defects in the group at the boundary of calculation cell [m^{-3}] (corresponding to the array index `mvv`), which must be relatively small, so is needed to control the correctness of calculations. <m> is the mean number of gas atoms in a gas bubble.

```
 15  n  visible   [---]         20         20         44 sdt= 1.809E-06
```

- The number of defects in the smallest visible clusters, and the swelling rate [%/dpa].

```
 16  SS for 1d Gl [m-2]  0.000E+00  0.000E+00  0.000E+00 sth= 1.928E-10
```

- The sink strength of defects for 1-D migrating crowdions [m^{-2}]; the standard rate theory estimate for the swelling rate in the sink-dominant regime [%/dpa].

```
 17  SS for 3d-i  [m-2]  1.201E+10  0.000E+00  2.892E+05 v+g= 7.840E+10
```

- The sink strength of defects for 3-D migrating interstitials [m^{-2}], and the effective sink strength for v+g reaction: i.e. the sink strength of single vacancies for gas atoms [m^{-2}].

```
 18  SS for 3d-v  [m-2]  5.577E+05  0.000E+00  3.377E+05 v+v= 3.089E+11
```

- The sink strength of defects for 3-D migrating vacancies [m^{-2}], and the effective sink strength for v+v reaction: i.e. the sink strength of single vacancies for vacancies [m^{-2}].

```
 19  Emission ivv [m-2]  1.207E-17  0.000E+00  1.208E-15 rod= 3.000E+14
```

- The emission rates from clusters [s^{-1}], and the dislocation line density [m^{-2}].

```
 20  N*<x>        [---]  7.442E-15  0.000E+00  1.809E-15 Sge= 3.785E-18
```

- The number of single defects accumulated in extended defects per lattice site [at^{-1}] (but for voids/ gas bubbles it is swelling in %), and the total number of gas atoms in bubbles [at^{-1}].

```
 21  Critical cl. [---]                    0          0 GBH= 0.000E+00
```

- Critical cluster size [number of defects] and grain boundary coverage by gas atoms [at^{-1}].

```
 22  Y fractions  [---]  6.767E-01  0.000E+00  3.233E-01
```

- Relative contributions of different defects to the total yield stress change.

```
 23  Y= 6.03E-03  [MPa]  dS= 1.207E-02 S= 2.400E+02
```

- Yield stress change and Yield stress in [MPa].

```
 24               [Vic]  dH= 4.469E-03 H= 1.350E+02
```

- Hardness increase and hardness in [Vickers].

```
 25  Critical nucleus    rcr= 0.000E+00 xcr= 0.000E+00 mcr= 0.000E+00
 26 L1D= 1.41E-20 gv/=4.45E+02 ssGB= 1.00E-03 sbi= 2.86E+05 sbv= 2.86E+05
 27 Ggb= 0.00E+00 Gbc=1.50E-14 Sw0 = 1.81E-15 SwR= 1.81E-15 dVV=-1.11E-16
 28 Gdi= 1.17-316 Gbe=7.37E-19 Sv0 = 0.00E+00 Sg0= 3.78E-18 dGG= 0.00E+00
 29 Gge= 3.50E-16 Gco=1.07E-10 Si0 = 7.44E-15
```

- Lines 25-29 are for random output, which changes often. In the present example, the main important parameters are (left column): Ggb – amount of gas at grain boundaries [at^{-1}], Gdi - amount of gas at dislocations [at^{-1}], Gge - amount of gas generated [at^{-1}], (second column) Gbc - amount of gas captured by gas bubbles, Gbe - amount of gas emitted from bubbles [at^{-1}], Gco characterizes conservation of gas = 1-(Ggb+Gdi+Gbc-Gbc)/Gge.

```
 30 GB sink strength for ivg=  6.735E+13  6.141E+13  0.000E+00
```

- The grain boundary sink strength for interstitials, vacancies and gas atoms, respectively [m^{-2}].

4.5. List of output files in alphabetic order

N	File name	Type	Short description
1	z_bevl.dat	txt	vacancy - vacancy loop binding energy [eV]
2	z_bewc.dat	txt	vacancy - void binding energy [eV]
3	z_bew3.dat	txt	vacancy – gas bubble binding energy [eV]
4	z_bewb.dat	txt	vacancy – gas bubble binding energy [eV]
5	z_emig.dat	txt	gas emission rates from gas bubbles[s^{-1}]
6	z_emiv.dat	txt	vacancy emission rates from gas bubbles [s^{-1}]
7	z_grid-wg.dat	txt	gas axis grid for gas bubbles
8	z_grid-wv.dat	txt	vacancy axis grid for gas bubbles
9	z_hard.dat	txt	hardening change [MPa]
10	z_harv.dat	txt	hardening change in Vickers
11	z_pcil.dat	txt	production rates of interstitial loops in cascades
12	z_pcvl.dat	txt	production rates of vacancy loops in cascades
13	z_pcwv.dat	txt	production rates of micro-voids in cascades
14	z_rezz.dat	txt	input data read from input file to check reading
15	z_sdif.dat	txt	final (current) size distribution of interstitial loops
16	z_sdil.dat	txt	all size distributions of interstitial loops
17	z_sdw3.dat	txt	final size distribution of gas bubbles for 3D plot
18	z_sdwf.dat	txt	final size distribution of gas bubbles/voids
19	z_sdws.dat	txt	2-D: gas-vacancy size distribution of gas bubbles for
20	z_sdwv.dat	txt	all size distributions of gas bubbles/voids
21	z_sdvf.dat	txt	final size distribution of vacancy loops
22	z_sdvl.dat	txt	all size distributions of vacancy loops
23	zm_conc.dat	txt	concentrations of mobile defects
24	zm_dens.dat	txt	densities of extended defects [m^{-3}]
25	zm_gasA.dat	txt	gas atoms accumulated at different sinks
26	zm_gasB.dat	txt	all information on bubbles
27	zm_intL.dat	txt	all information on interstitial loops
28	zm_radi.dat	txt	radii of extended defects [nm]
29	zm_swss.dat	txt	swelling and sink strengths of various defects
30	zm_vacL.dat	txt	all information on vacancy loops
31	zz_age_ct.dat	binary	file for aging continuation
32	zz_igr_ct.dat	binary	file for calculation of surface irradiation
33	zz_irr_ct.dat	binary	file for irradiation continuation

4.6. Detailed description of the output files

1 z_bevl.dat - vacancy - vacancy loop binding energy [eV].

2 z_bewc.dat - vacancy – void binding energy [eV].

3 z_bew3.dat - vacancy – gas bubble binding energy [eV] for 3D graph.

xgas - number of gas atoms in gas bubble;

xvac - number of vacancies in loop/void/gas bubble;

Eb(eV) - binding energy of a vacancy with a gas bubble/loop/void [eV].

4 z_bewb.dat - vacancy – gas bubble binding energy [eV].

vac - number of vacancies in a gas bubble;
g0,g1... - correspondingly 0,1 ... gas atoms in gas bubble.

5 z_emig.dat - gas emission rates from gas bubbles [s^{-1}].

Same as above in file 04.

6 z_emiv.dat - vacancy emission rates from gas bubbles [s^{-1}].

Same as above in file 04.

7 z_grid-wg.dat - gas axis grid for gas bubbles.

Same as below in file 08.

8 z_grid-wv.dat - vacancy axis grid for gas bubbles.

N - index of the array element (group);
X_def - number of defects (gas or vacancies) in gas bubble;
R_nm - gas bubble radius [nm].

9 z_hard.dat - hardening [MPa].

10 z_harv.dat - hardening in Vickers.

11 z_pcil.dat - production rates of interstitial loops in cascades.

n_int - number of interstitials;
Rate - production rate [s^{-1}];
Comment: the mean value $<x>$ is calculated from 2 to maximum.

12 z_pcvl.dat - production rates of vacancy loops in cascades.

Same as above in file 11.

13 z_pcwv.dat - production rates of micro-voids in cascades.

Same as above in file 11.

14 z_rezz.dat - input data read from input file to check reading.

15 z_sdif.dat - final size distribution of interstitial loops.

R_nm - interstitial loop radius [nm];
abs_f(R) - abs of size distribution to present in log scales;
f(R) - size distribution in *R* space [m^{-3} nm^{-1}];
n_def - mean (over group) number of defects in a cluster;
f(n_vac) - size distribution in *x* space [at^{-1}];
slope - slope of *x*-space size distribution in group [at^{-1}].

16 z_sdil.dat - all size distributions of interstitial loops.

Same as above in file 15 but for different irradiation doses.

17 z_sdw3.dat - final size distribution of bubbles for 3D plot.

1st column - number of gas atoms;
2nd column - gas bubble radius [nm];
3rd column - gas bubble density in *R*-space [$m^{-3}nm^{-1}$].

18 z_sdwf.dat - final size distribution of gas bubbles/voids.

R_nm - void/gas bubble radius [nm];
abs_f(R) - absolute values of size distribution to plot in log scales;
f(R) - size distribution in *R* space [$m^{-3}nm^{-1}$];
n_vac - mean (over group) number of vacancies in a cluster;

f(n_vac) - size distribution in *x* space [at^{-1}];
slope - slope of x-space distribution inside the group [at^{-1}];
m/x - number of gas atoms to number of vacancies ratio;
P_GPa - gas pressure [GPa] averaged over group;
Z - gas compressibility, characterizes gas non-ideality;
r/RWZ - bubble radius/Wigner-Zeitz radius.

19 z_sdws.dat - 2-D: gas-vacancy size distribution of gas bubbles for different doses

Two-dimensional size distributions in x space for different irradiation doses; the number of gas atoms increases from top to bottom and the vacancy numbers increases from left to right; the densities are in [at^{-1}].

20 z_sdwv.dat - all size distributions of bubbles/voids.

Same as for z_sdwf.dat but for different irradiation doses.

21 z_sdvf.dat - final size distribution of vacancy loops.

22 z_sdvl.dat - all size distributions of vacancy loops.

23 zm_conc.dat - concentrations of mobile defects.

Dose/Time - either irradiation dose [dpa] or time in [s];
Ci - interstitial concentration [at^{-1}];
Cv - vacancy concentration [at^{-1}];
CGas - gas atom concentration [at^{-1}];
Ccrow - crowdion concentration [at^{-1}].

24 zm_dens.dat - densities of extended defects [m^{-3}].

Dose/Time - either irradiation dose [dpa] or time [s];
N_i_loop - number density of interstitial loops bigger than 2i;
Nn_i_loop - number density of visible interstitial loops;
N_v_loop - number density of vacancy loops bigger than 2v;
Nn_v_loop - number density of visible vacancy loops;
N_void - number density of voids bigger than 2v;
Nn_void - number density of visible voids.

25 zm_gasA.dat - gas atoms at different sinks.

Dose/Time - either irradiation dose [dpa] or time [s];
CGas - freely migrating gas [at^{-1}];
Gas_bubb - in bubbles [at^{-1}];
Gas_dsl - at dislocations [at^{-1}];
Gas_GB - at grain boundaries [at^{-1}];
GB_Cover - grain boundary coverage with gas atoms.
G_Gas_s-1 - generation rate [s^{-1}];
<mgas> - mean number of gas at per bubble.

26 zm_gasB.dat - all information on bubbles.

Dose/Time - either irradiation dose [dpa] or time [s];
N_m-3 - bubble number density [m^{-3}];
R_nm - bubble mean radius [nm];
Swelling_% - swelling due to bubbles [%]=[100.*at^{-1}];
SS_m-2 - bubble sink strength for freely-migrating interstitials [m^{-2}];

Nn_m-3 - number density of visible bubbles [m^{-3}];
Rn_nm - mean radius of visible bubbles [nm];
<mgas> - mean number of gas atoms at per bubble;
DenZ_nm - mean distance between bubbles [nm].

27 zm_intL.dat - all information on interstitial loops.

Dose/Time - either irradiation dose in dpa or time [s];
N_m-3 - loop number density [m^{-3}];
R_nm - loop mean radius [nm];
SNdeff - total defects accumulated in loops [at^{-1}];
SS_m-2 - sink strength for freely-migrating interstitials [m^{-2}];
Nn_m-3 - number density of visible loops [m^{-3}];
Rn_nm - mean radius of visible loops [nm].

28 zm_radi.dat - radii of extended defects [nm].

Dose/Time - either irradiation dose in [dpa] or time in [s];
R_i_loop - mean radius of interstitial loops bigger than 2i;
Rn_i_loop - mean radius of visible interstitial loops;
R_v_loop - mean radius of vacancy loops bigger than 2v;
Rn_v_loop - mean radius of visible vacancy loops;
R_void - mean radius of voids/bubbles bigger than 2v;
Rn_void - mean radius of visible voids/bubbles;
RWZ_void - Wigner-Zeitz cell radius for 3-D migrating defects.

29 zm_swss.dat - swelling and sink strengths.

Dose/Time - either irradiation dose [dpa] or time [s];
I_in_loops - total number of interstitial in loops [at^{-1}];
V_in_loop - total number of vacancies in loops [at^{-1}];
Swelling_% - swelling [%]=[100 at^{-1}];
SW_GB - not used in the current version of the code.
SSi_i_lps - sink strength of interstitial loops for interstitials [m^{-2}];
SSi_v_lps - sink strength of vacancy loops for interstitials [m^{-2}];
SSi_voids - sink strength of voids/bubbles for interstitials [m^{-2}];
rod_m-2 - dislocation density [m^{-2}];
MFP3d_nm - mean-free path of freely-migrating defects [m];
S_dot_%/dpa - swelling rate [at^{-1}/dpa].

30 zm_vacL.dat - all information on vacancy loops.

31-33 see section 4.7 below

4.7. Binary files used to save intermediate state for further calculation or restarts

4.7.1. (31) zz_age_ct.dat: continuation of aging

This file contains data on current time, concentrations of mobile species, size distribution functions of sessile defects: voids/bubbles, loops and dislocations, and some other information, necessary to continue aging calculation to longer time.

4.7.2. (32) zz_igr_ct.dat: surface irradiation after bulk irradiation

This file is not generated and used in the current version of the code.

4.7.3. (33) zz_irr_ct.dat: continuation of irradiation

The file contains data on current time, concentrations of mobile species, size distribution functions of sessile defects voids/bubbles, loops and dislocations, and some other information, necessary to continue calculation of irradiation to a higher irradiation dose; and also to start new calculation of aging if irradiated sample.

5. Summary of Status and Future Work

The new and more comprehensive microstructural model has been built and debugged. The initial predictions of the model provide reasonable agreement with microstructural observations using only a nominal set of material properties for austenitic stainless steel. Since the cavity evolution component describes a two-dimensional vacancy-helium phase space, the computational requirements have increased substantially from simpler models. The longer computer run times, along with the increase in the number of physical parameters required, make model calibration a more challenging exercise.

Work during the next phase of the project will initially focus on a detailed model calibration effort which will employ the available relevant microstructural data from post-irradiation examination of LWR components. An extensive series of simulations will be carried out to determine the sensitivity of the model's predictions to the full range of required irradiation and materials parameters. This will also include an assessment of the relevance of in-cascade point defect clustering and the rapid one-dimensional migration of small interstitial clusters as observed in molecular dynamics simulations. Since there is only a limited amount of such data, the calibration data set will also include data from other irradiation environments, including higher-temperature test reactor irradiations and ion irradiations. Since ion irradiations are conducted at much higher damage rates, the use of this data will involve an assessment of the model's ability to capture the effects of damage rate; this will increase the usefulness of the model to the LWRS and other nuclear materials programs.

The parametric assessments, including the impact of their related uncertainties, will enable us to determine a best estimate of all model input parameters. These parameters will be used develop a set of bounding calculations for the swelling that can be reasonably expected over the lifetime of LWR internal component fabricated from austenitic stainless steel. Information on the associated dislocation evolution can be used to estimate mechanical property changes.

Finally, although it was not a stated goal of the current project, it should be straight forward to extend the model to other materials and properties. For example, the dynamic dislocation model should make it possible to simulate irradiation creep, and the application of the model to ferritic and ferritic-martensitic steels should only require the adjustment of material parameters.

References

[1] R. E. Stoller, A. V. Barashev, and S. I. Golubov, "Low-temperature Swelling in LWR Internal Components: Current Data and Modeling Assessment," ORNL/LTR-2012/390, Oak Ridge National Laboratory, September 2012.

[2] R. E. Stoller, A. V. Barashev, and S. I. Golubov, "The Influence of Helium on Low-temperature Swelling in LWR Internal Components," ORNL/LTR-2013/200, Oak Ridge National Laboratory, September 2013.

[3] R. E. Stoller, A. V. Barashev, and S. I. Golubov, "Cavity Nucleation Under Irradiation Conditions Typical of LWR Internal Components," ORNL/LTR-2013/487, Oak Ridge National Laboratory, May 2013.

[4] S.I. Golubov, A.M. Ovcharenko, A.V. Barashev, and B.N. Singh, "Grouping method for the approximate solution of a kinetic equation describing the evolution of point-defect clusters," Philos. Mag. A. 81 (2001) 643-658.

[5] S.I. Golubov, R.E. Stoller, and S.J. Zinkle, "Nucleation and growth of helium-vacancy clusters in irradiated metals. Part. I. A group method for an approximate solution of two dimensional kinetic equations describing evolution of point defect clusters," Fusion materials semi-annual progress report for period ending December 31, 2002, DOE/ER-0313/33, US Department of Energy, pp. 155-180.

[6] S.I. Golubov, R.E. Stoller, and S.J. Zinkle, "Nucleation and growth of helium-vacancy clusters in irradiated metals. Part II. A grouping method for an approximate solution of two dimensional kinetic equations describing evolution of point defect clusters taking into account Brownian motion of the clusters," Fusion materials semi-annual progress report for period ending December 31, 2003, DOE/ER-0313/35, US Department of Energy, pp. 214-231.

[7] S.I. Golubov, R.E. Stoller, and S.J. Zinkle, "An improved solution to the kinetic equations describing defect cluster dynamics during irradiation or thermal ageing," GEN-IV Nuclear Energy System, ORNL-GEN4/LTR-06-012, Oak Ridge National Laboratory, 2006.

[8] S.I. Golubov, R.E. Stoller, S.J. Zinkle, and A.M. Ovcharenko, "Kinetics of coarsening of helium bubbles during implantation and post-implantation annealing," J. Nucl. Mater. 361 (2007) 149-159.

[9] A.C. Hindmarsh, "LSODE and LSODI, two new initial value ordinary differential equation solvers," ACM SIGNUM Newsletter 15, no. 4 (1980) 10-11.

[10] A.C. Hindmarsh, "ODEPACK: A Systematized Collection of ODE solvers," Scientific Computing, R.S. Stepleman, et al., eds., North Holland Publishing Co., New York, (1983), pp. 5544.

[11] K. Radhakrishnan and A.C. Hindmarsh, "Description and use of LSODE, the Livermore Solver for Ordinary Differential Equations," UCRL-ID-113855, Lawrence Livermore National Laboratory, NASA Reference Publication 1327, 1993.

[12] N.F. Carnahan and K.E. Starling, "Equation of State for Nonattracting Rigid Spheres," J. Chem. Phys. 51 (1969) 635-636.

[13] R.E. Stoller, unpublished work.

[14] R. Manzke, W. Jäger, H. Trinkaus, G. Crecelius, and_R. Zeller, *Solid State Communications* 44 (1982) 481.

[15] A. Si-Ahmed and W. G. Wolfer, "Effect of Radiation-induced Segregation on Void Nucleation," Effects of Radiation on Materials, ASTM STP 782, H.R. Brager and J.S. Perrin Eds., American Society for Testing and Materials, Philadelphia, 1982, pp. 1008-1022.

[16] M.J. Norgett, M.T. Robinson, and I.M. Torrens, "A Proposed Method of Calculating Displacement Dose Rates," Nucl. Eng. Des. 33 (1975) 50-54.

[17] L.R. Greenwood, D.W. Kneff, R.P. Skowronski, and F.M. Mann, "A Comparison of Measured and Calculated Helium Production in Nickel Using Newly Evaluated Neutron Cross Sections for 59Ni," J. Nucl. Mater. 122-123 (1984) 1002-1010.

[18] R.E. Stoller and G.R. Odette, "A Composite Model of Microstructural Evolution in Austenitic Stainless Steel Under Fast Neutron Irradiation," Radiation Induced Changes in Microstructure: 13th International Symposium, ASTM STP 955, F.A. Garner, N.H. Packan, and A.S. Kumar, Eds., American Society for Testing and Materials, Philadelphia, 1987, pp. 371-392.